

# Performance Analysis of Intelligent Reflecting Surface Assisted Opportunistic Communications

L. Yashvanth, *Graduate Student Member, IEEE*, Chandra R. Murthy, *Senior Member, IEEE*

**Abstract**—Intelligent reflecting surfaces (IRSs) are a promising technology for enhancing coverage and spectral efficiency, especially in the millimeter wave (mmWave) bands. Existing approaches to leverage the benefits of IRS involve the use of a resource-intensive channel estimation step followed by a computationally expensive algorithm to optimize the reflection coefficients at the IRS. In this work, we present and analyze several alternative schemes, where the phase configuration of the IRS is randomized and multi-user diversity is exploited to opportunistically select the best user at each point in time for data transmission. We show that the throughput of an IRS assisted opportunistic communication (OC) system asymptotically converges to the optimal beamforming-based throughput under fair allocation of resources, as the number of users gets large. We also introduce schemes that enhance the rate of convergence of the OC rate to the beamforming rate with the number of users. For all the proposed schemes, we derive the scaling law of the throughput in terms of the system parameters, as the number of users gets large. Following this, we extend the setup to wideband channels via an orthogonal frequency division multiplexing (OFDM) system and discuss two OC schemes in an IRS assisted setting that clearly elucidate the superior performance that IRS aided OC systems can offer over conventional systems, at very low implementation cost and complexity.

**Index Terms**—Intelligent reflecting surfaces, opportunistic communication, OFDM.

## I. INTRODUCTION

Intelligent Reflecting Surfaces (IRSs) have become a topic of active research for enhancing the performance of next generation wireless communication systems in the millimeter wave (mmWave) bands. An IRS consists of passive elements made out of meta-materials that can be tuned to offer a wide range of load impedances using a PIN diode. Using this, each element of the IRS can be tuned to have a different reflection coefficient, and thereby enable the IRS to reflect the incoming signals in any desired direction [1]–[3]. In turn, this can be used to extend the range, improve the signal strength and even allow mmWave signals to go around obstacles [4]. However, realizing these benefits requires resource-intensive channel estimation (the training overhead required scales linearly with the number of IRS elements) followed by solving a computationally expensive optimization problem to determine the phase angle configuration at the IRS. In this work, we consider an alternative approach, first proposed in [5], where the phase configuration of the IRS is set randomly in each slot. This only requires a short training signal for estimating

The authors are with the Department of Electrical Communication Engineering, Indian Institute of Science, Bangalore, India 560 012. (E-mails: {yashvanth, cmurthy}@iisc.ac.in). This work was supported in part by the Qualcomm Innovation Fellowship, 2021.

the received signal power at the users, followed by feedback-based selection of the best user in each slot for subsequent data transmission. Multi-user diversity ensures that at least one user will see a good channel in the randomly chosen phase configuration. Thus, it greatly reduces the training and optimization overheads of IRS, while still reaping its benefits.

Despite its short history, significant work has gone into the design and optimization of IRS-aided communication systems. Here, we briefly summarize the existing literature, in order to place the contributions of this paper in context. In [6], the authors show that an IRS can create a virtual line-of-sight (LoS) path between the base station (BS) and user, leading to improved coverage and SNR in mmWave systems. In [7], it is shown that the received SNR increases quadratically with the number of IRS elements, provided the phase configuration of the IRS is set optimally to ensure coherent combining of the signal at the receiver location. Also, since the IRS is passive in nature, it incurs only a little additional power to program its phase configuration [8]. In [9], the authors propose a joint active and passive beamforming algorithm at the BS and IRS, respectively, to maximize the weighted sum rate of an IRS-aided multiple-input single-output (MISO) system. On similar lines, the spectral efficiency (SE) and energy efficiency (EE) of an IRS assisted MISO system is analyzed in [10]. IRSs have also been used to create nulling patterns and cancel the interference in specific directions, which helps to reduce the transmission power margin [3]. IRS phase optimization in the context of multiple-input multiple-output (MIMO) and orthogonal frequency division multiplexing (OFDM) systems have been studied in [11]–[15], and the list of potential applications of IRS continues to grow [3], [16]–[18].

All of the above mentioned works describe and solve a complex phase optimization problem, which are computationally intensive and difficult to implement in practical real-time systems. Further, this optimization becomes even more complex in the context of OFDM systems, as it requires one to optimize the IRS jointly across all the OFDM subcarriers. More importantly, these phase optimization algorithms work on the premise of the availability of accurate channel state information (CSI) of the links between the BS and the user through every IRS element. Elegant methods for channel estimation in IRS aided systems are described in [19], [20], but in all these schemes, the channel estimation overhead scales linearly with the number of IRS elements. The time, energy and resource utilization for channel estimation can quickly erase much of the benefits offered by the IRS. One approach to mitigate this loss is to exploit structure in the channel model to estimate the channel with lower overhead [21]–[23], but

these approaches trade-off the reduction in overhead with more complex channel estimation algorithms, thereby substantially increasing the computational cost. In addition, the complexity of the overall algorithm increases with the resolution with which phase shifts are configured [24]. Thus, regardless of how they are implemented, the use of IRS incurs substantial computational and training overheads in order to fully reap their professed benefits. Furthermore, since the IRS is passive, these optimization algorithms have to run at the BS, and a dedicated control link from the BS to the IRS is needed to communicate the phase configuration information to the IRS. As the number of IRS elements increases, this becomes an additional bottleneck, as the control link overhead also scales with the number of IRS elements [3].

In the context of the above, it is pertinent to explore whether one can circumvent the channel estimation and phase optimization overheads and still obtain most of the benefits of an IRS assisted system. An interesting approach, first explored the context of IRS in [5], is to randomly select the phase configuration at the IRS and make the communication opportunistic in nature. In opportunistic communications (OC), the central theme is to exploit multi-user diversity and serve users who witness the best instantaneous channel condition at every point in time. As a consequence, with high probability, deep fade events are avoided at any given user, enhancing the average throughput of the system. OC based schemes, pioneered in [25], [26] and nicely summarized in the survey paper [27], are attractive because they can greatly enhance the system throughput with very low complexity. In [5], the phase angles of the reflection coefficients at the IRS elements are drawn uniformly and independently from the interval  $[0, 2\pi]$ . Due to this, the number of users needed to achieve a performance comparable to coherent beamforming increases rapidly with the number of IRS elements. As a result, the method is applicable only when the number of IRS elements is small. In practice, one would like to use an IRS with a much larger number of elements, in order to achieve an appreciable coherent beamforming gain.

In this paper, we make progress on the IRS-assisted OC paradigm by analyzing the convergence behavior of the data rate achieved as the number of users increase. Further, by exploiting the structure in the channel, we propose alternative schemes for random phase selection that improves the convergence rate. The latter allows us to extract the benefits of the IRS while avoiding the high training and computational overheads, and achieve near-optimal coherent beamforming performance without requiring a large number of users in the system. The specific contributions of our work are as follows:

- We analyze the throughput of several IRS-assisted OC schemes for slowly varying narrowband wireless channels. As an enhancement to the basic OC scheme in [5], we exploit the fast switching time of IRS configurations to leverage additional reflection diversity from the IRS. We show that this helps to reduce the number of users required to obtain near-optimal coherent beamforming throughput. We also analytically characterize the throughput achievable by this scheme in Theorem 2, and provide insights. (See Sec. III-B.)

- Next, we account for channel structure in the IRS aided system and design OC schemes that can converge to the coherent beamforming rate with far fewer users. We analytically derive the scaling laws for this scheme, in terms of how the throughput scales with the number of IRS elements and users in the system. In Proposition 1, we show that the throughput of this scheme can even surpass the performance of the scheme that involves IRS optimization techniques, due to the lack of multi-user diversity gain in the latter approach. (See Sec. III-C.)
- We extend the OC schemes to IRS aided systems with slowly-varying wideband wireless channels. Specifically, we consider an OFDM system and discuss two OC schemes, namely, single user OFDM where we schedule a single user across all subcarriers, and orthogonal frequency division multiple access (OFDMA) where multiple users are potentially scheduled across the subcarriers. We derive the sum throughput scaling laws in Theorems 3 and 4 for the two schemes, and provide interesting insights about these systems. (See Sec. IV.)

We empirically illustrate the advantages of the OC schemes developed, and compare them with existing approaches, via Monte Carlo simulations, in Sec. V. The results show that IRS-aided OC significantly outperforms OC in the absence of an IRS, for e.g., BS-assisted OC [25]. Specifically, the throughput of IRS aided OC grows logarithmically with  $N$ , whereas such growth is not possible in BS assisted OC due to the power constraint at transmitter, which eventually limits the maximum achievable multi-user diversity gains. Secondly, in order to achieve a given multi-user diversity gain from the basic scheme of IRS aided OC, the number of users must scale exponentially with the number of IRS elements. For e.g., the achieved OC rate out of an 4-element IRS system is offset by 150% from beamforming rate in the low-user regime, but in an 8-element IRS system, the gap increases to 175%. In contrast, the reflection diversity enhanced scheme lowers the offset to 47% and 60% in 4- and 8-element IRS systems, respectively. Finally, as an additional boost, the offsets above reduce to 10% and 11%, respectively, in the channel model aware IRS assisted OC scheme. Also, the channel model aware OC scheme is within a small offset (18%) with a modest number of users ( $\approx 50$ ), even when the number of IRS elements is as large as 1024. Thus, IRS aided OC is a promising approach for exploiting the benefits of IRS-aided systems without incurring the cost of training, phase angle optimization, and communication to the IRS.

*Notation:* Boldface lower and upper case letters denote vectors and matrices.  $[N]$  stands for the set of natural numbers from 1 to  $N$ ;  $(\cdot)^T, (\cdot)^H$  denote transpose and Hermitian (conjugate transpose) of a vector/matrix;  $|\cdot|, \angle \cdot$  stand for the magnitude and phase of a complex number (vector);  $\lceil \cdot \rceil, \lfloor \cdot \rfloor$  denote the ceiling and floor functions; and  $\|\cdot\|_p$  denotes the  $\ell_p$  vector norm.  $\mathcal{CN}(\mu, \Sigma)$  denotes a circularly symmetric complex Gaussian random vector with mean vector  $\mu$  and covariance matrix  $\Sigma$ ;  $\mathcal{U}(\phi_0, \phi_1)$  denotes a uniformly distributed random variable with support  $[\phi_0, \phi_1]$ ,  $\exp(\lambda)$  denotes an exponentially distributed random variable with parameter

$\lambda$ , i.i.d. stands for independent and identically distributed,  $Pr(\cdot)$  refers to the probability measure, and  $\mathbb{E}[\cdot]$  refers to the statistical expectation.  $\mathcal{O}(\cdot)$  is the Landau's Big-O notation.

In the next section, we briefly present some preliminary background on OC schemes, which will serve as our point of departure in this paper.

## II. PRELIMINARIES

Opportunistic communication schemes exploit the variation of the fading channels across users in order to improve the throughput of a multi-user system. For example, in max-rate based scheduling [27], the BS sends a common pilot signal to all the users in the system, and the users measure the received SNR. The BS then collects feedback from the user who witnesses the highest SNR,<sup>1</sup> and schedules data to that user in the rest of the slot. That is, in a  $K$  user system, the BS serves user  $k^*$  at time  $t$ , where

$$k^* = \arg \max_{k \in [K]} |h_k(t)|^2,$$

with  $h_k(t)$  denoting the channel seen by user  $k$  at time  $t$ . However, this scheme is unfair to users located far away from the BS due to their higher path loss. An alternative is to consider the proportional fair (PF) scheduling scheme, which provides a trade-off between fairness and system throughput [25]. The PF scheduler serves user  $k^*$  at time  $t$  such that

$$k^* = \arg \max_{k \in [K]} \frac{R_k(t)}{T_k(t)}, \quad (1)$$

where  $R_k(t) = \log_2 \left( 1 + \frac{P|h_k(t)|^2}{\sigma^2} \right)$  is the achievable rate<sup>2</sup> of user  $k$  in the current time slot,  $P$  is the transmit power at the BS,  $\sigma^2$  is the noise variance at the user, and  $T_k(t)$  captures the long-term average throughput of user  $k$ . It is updated as

$$T_k(t+1) = \begin{cases} \left(1 - \frac{1}{T_c}\right) T_k(t) + \frac{1}{T_c} R_k(t), & k = k^*, \\ \left(1 - \frac{1}{T_c}\right) T_k(t), & k \neq k^*. \end{cases} \quad (2)$$

Here, the variable  $T_c$  represents the length of a window that captures the tolerable latency of the application and dictates the trade-off between fairness and throughput. Going forward, we will refer to the term  $\frac{R_k(t)}{T_k(t)}$  as the PF metric.

A simple illustration of exploiting multi-user diversity through opportunistic scheduling based on the PF scheduler is shown in Fig. 1 for various values of  $T_c$ . We consider a time-varying channel across time slots modeled as a Gauss-Markov process, i.e., the channel at user  $k$  varies as

$$h_k(t) = \alpha h_k(t-1) + \sqrt{1-\alpha^2} v_k(t), \quad (3)$$

where  $\alpha$  dictates the correlation of channel coefficients across time slots and  $v_k(t) \sim \mathcal{CN}(0, 1)$  is an innovation process.

Further, the performance of the OC scheme is compared with a non-opportunistic scheduling scheme, namely, round-robin time division multiple access (TDMA).

<sup>1</sup>We note that various timer-based and splitting based schemes can be used to identify the best user with low overhead [28], [29].

<sup>2</sup>In this paper, we use rate and throughput interchangeably.

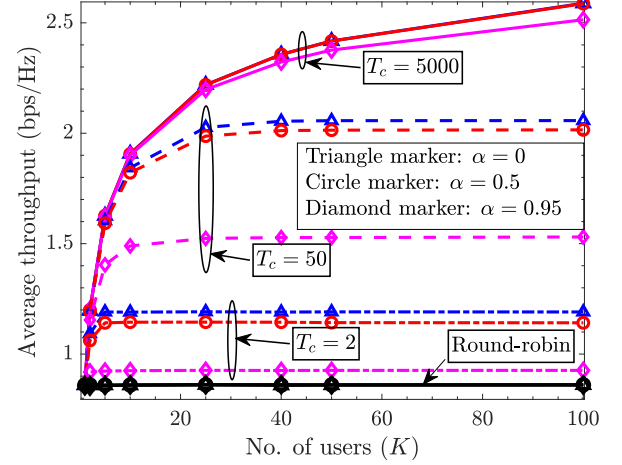


Fig. 1: Throughput achieved via PF scheduling.

As can be seen from the figure, the average throughput of the system at higher  $T_c$  grows substantially with the number of users. This marks the rate-constrained regime, where the instantaneous rate is the primary factor determining which user gets scheduled (the system still offers fairness, but only over very large time-scales). Thus, for large  $T_c$ , the PF scheduler is approximately the same as a max-rate scheduler, and the throughput achieved by the PF scheduler approaches that achieved by the max-rate scheduler as  $T_c$  goes to infinity. On the other hand, at lower  $T_c$ , the average throughput has negligible improvement after a few users, indicating that this is a fairness-constrained regime where users are selected in a nearly round-robin fashion to ensure short-term fairness. On the other hand, for a given choice of  $T_c$ , opportunistic scheduling performs better for lower values of  $\alpha$  (representing a fast-fading scenario) compared to higher values (representing slow-fading scenarios). This is because, in fast-fading environments, the rate of channel fluctuations are enhanced, which improves the performance of opportunistic scheduling schemes. We note that a similar enhancement of the rate of channel fluctuations can be obtained by choosing different, random phase configurations at an IRS. This has the additional advantage that the fluctuations induced by the IRS increases with the number of elements. This motivates us to take a fresh look at the opportunistic scheduling schemes in IRS-assisted scenarios. Specifically, we analyze the scaling of throughput achieved in IRS-assisted OC schemes and show that one can obtain the benefits of using an IRS over conventional systems with low overhead and complexity by obviating the need for CSI acquisition, IRS phase optimization and feedback between the BS and the IRS.

## III. SINGLE IRS ASSISTED OPPORTUNISTIC USER SCHEDULING FOR NARROWBAND CHANNELS

In this section, we present three OC schemes in a single IRS assisted setting, for narrowband channels. We consider a single cell containing a BS equipped with one antenna serving  $K$  single antenna users. An IRS equipped with  $N$

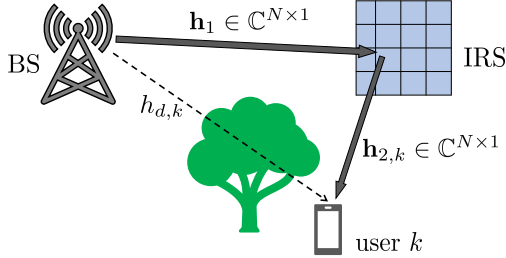


Fig. 2: A single IRS assisted wireless system.

reflecting elements is deployed at a suitable location in the radio propagation environment, as shown in Fig. 2.

### A. IRS-Enhanced Multi-user Diversity

1) *Channel Model*: The signal transmitted by the BS reaches each the user via a direct path as well as via the IRS. Thus, the effective downlink channel seen by user  $k$  (at time slot  $t$ ), denoted by  $h_k$  (we omit the dependence on  $t$  for notational brevity), is given by

$$h_k = \sqrt{\beta_{r,k}} \mathbf{h}_{2,k}^H \Theta \mathbf{h}_1 + \sqrt{\beta_{d,k}} h_{d,k}, \quad (4)$$

where  $\mathbf{h}_{2,k} \in \mathbb{C}^{N \times 1}$  and  $\mathbf{h}_1 \in \mathbb{C}^{N \times 1}$  represent the channels between the IRS and user  $k$  and between the BS and IRS, respectively, and  $h_{d,k}$  denotes the direct non-IRS channel between the BS and user  $k$ . We model  $\mathbf{h}_1 \sim \mathcal{CN}(\mathbf{0}, \mathbf{I})$ ,  $\mathbf{h}_{2,k} \stackrel{\text{i.i.d.}}{\sim} \mathcal{CN}(\mathbf{0}, \mathbf{I})$  and  $h_{d,k} \stackrel{\text{i.i.d.}}{\sim} \mathcal{CN}(0, 1)$  across all users. Further,  $\beta_{r,k}$  and  $\beta_{d,k}$  represent the path loss between the BS and user  $k$  through the IRS and direct paths, respectively. The diagonal matrix  $\Theta \in \mathbb{C}^{N \times N}$  contains the reflection coefficients programmed at the IRS, with each diagonal element being of the form  $e^{j\theta_i}$ , where  $\theta_i \in [0, 2\pi]$  is the phase angle of the reflection coefficient at the  $i$ th IRS element. The signal received at every user is corrupted by AWGN  $\stackrel{\text{i.i.d.}}{\sim} \mathcal{CN}(0, \sigma^2)$ .

2) *Scheme for IRS-Enhanced Multi-user Diversity*: In every time slot, the IRS chooses a random phase configuration. As a consequence, the effective channels seen by the users change from slot to slot. The BS transmits a pilot signal in the downlink at the start of the slot. The users measure the SNR from the received pilot signal, and compute their respective PF metrics. The user with the highest PF metric feeds back its identity to the BS using a timer or splitting based scheme,<sup>3</sup> and the BS schedules that user for data transmission for the rest of the slot.

In the above scheme, as the number of users in the system grows, the randomly chosen IRS configuration is likely to be close to the beamforming (BF) configuration for at least one of the users in the system, similar to [25]. Note that, in this scheme, there is no communication from the BS to

<sup>3</sup>These timer or splitting-based schemes, when well designed, can identify the best user within 2 or 3 (mini-)slots on average. The users generate feedback to the BS based on their channel-utility metric (e.g., a timer that expires after a time that is inversely proportional to the SNR), ensuring that the BS can identify the best user with very low feedback overhead even as  $K \rightarrow \infty$  [28], [29]. Since the average overhead of a timer based feedback scheme is small compared to the time slot duration, we ignore its effect in this paper.

IRS, making it attractive from an implementation perspective. Thus, the benefits of an optimized IRS can be readily obtained without requiring careful optimization of the IRS, provided there are a large number of users in the system and the multi-user diversity gain is exploited.

We begin our discussion with the following theorem on the performance of an IRS that adopts a beamforming configuration to a given user, which will serve as a benchmark for evaluating the OC based schemes. Its proof is available in [5].

**Theorem 1.** *The rate achieved by user  $k$  in an IRS aided system under the beamforming configuration is  $R_k^{BF} =$*

$$\log_2 \left( 1 + \frac{P}{\sigma^2} \left| \sqrt{\beta_{r,k}} \sum_{n=1}^N |h_{1,n} h_{2,k,n}| e^{j\angle h_{d,k}} + \sqrt{\beta_{d,k}} h_{d,k} \right|^2 \right), \quad (5)$$

with the beamforming configuration at the IRS given by

$$\theta_{n,k}^* = \angle h_{d,k} - \angle (h_{1,n} + h_{2,k,n}), \quad n = 1, \dots, N. \quad (6)$$

The above Theorem quantifies the gain that an IRS can offer compared to a system in the absence of IRS. However, achieving the rate in (5) requires the knowledge of the CSI through every IRS element whose complexity scales linearly with the number of elements, as stated earlier.

Next, consider the system where the phase of every IRS element is selected uniformly at random in the interval  $[0, 2\pi]$  in each slot, and the user with the best PF metric is selected for transmission. We define the average rate achieved by the randomly configured IRS assisted system to be  $R^{(K)} = \mathbb{E} [\log_2 (1 + P|h_{k^*}|^2 / \sigma^2)]$ , where  $k^*$  is the user selected for transmission in time slot  $t$ , and the expectation is taken over the randomness in the phase configuration. We have the following Lemma.

**Lemma 1** ([5]). *Under PF scheduling, with  $T_c \rightarrow \infty$ , the average rate of the randomly configured IRS assisted system almost surely converges to the average rate achievable in the beamforming configuration under fair resource allocation across users, i.e.,*

$$\lim_{K \rightarrow \infty} \left( R^{(K)} - \frac{1}{K} \sum_{k=1}^K R_k^{BF} \right) = 0. \quad (7)$$

Note that, in (7), the factor  $\frac{1}{K}$  in the second term on left hand side accounts for the fairness ensured by the system.

**Remark 1.** *Let us compute the scaling of the number of users  $K$  with the number of IRS elements  $N$ , such that, with a given (fixed) probability, a randomly selected phase configuration  $\Theta$  at the IRS is nearly in beamforming configuration for at least one user. Consider an arbitrary user, and define the event  $\mathcal{E}_i \triangleq \{\theta_i \in [\theta_i^* - \epsilon, \theta_i^* + \epsilon]\}$ , where  $\theta_i^*$  is the phase angle required for the  $i$ th element of the IRS to be in beamforming configuration for that user. Since the phase angles at the IRS are chosen as  $\theta_i \stackrel{\text{i.i.d.}}{\sim} \mathcal{U}[0, 2\pi]$ , if we define  $\mathcal{E} \triangleq \bigcap_{i=1}^N \mathcal{E}_i$ , we have  $\Pr(\mathcal{E}) = (\epsilon/\pi)^N$ . Then, the probability that at least one*

user in a  $K$ -user system sees an IRS phase configuration that is within  $\epsilon$  distance of its beamforming configuration is

$$P_{\text{succ}} = 1 - \left(1 - \left(\frac{\epsilon}{\pi}\right)^N\right)^K. \quad (8)$$

Hence, in order to have a fixed probability of success via i.i.d. randomly selected phase configurations, the number of users must scale with  $N$  as

$$K \geq \frac{\log(1 - P_{\text{succ}})}{\log\left(1 - \left(\frac{\epsilon}{\pi}\right)^N\right)}. \quad (9)$$

In particular, if  $\epsilon/\pi \ll 1$ , (9) can be approximated as  $K \geq (-\log(1 - P_{\text{succ}}))(\pi/\epsilon)^N$ . That is, the i.i.d. phase configuration scheme constrains the number of IRS elements that can be deployed when the number of users is limited.<sup>4</sup> In the next subsections, we present and analyze schemes that improve the rate of convergence of  $R^{(K)}$  to  $\frac{1}{K} \sum_{k=1}^K R_k^{\text{BF}}$ .

### B. IRS-Enhanced Multi-user Diversity Aided with Reflection Diversity

In the preceding subsection, an elementary scheme for an IRS assisted system exploiting multi-user diversity was discussed. This scheme becomes advantageous when the number of users grows exponentially with the number of IRS elements. However, when users are small in number, the effect of multi-user diversity is naturally less pronounced. In this subsection, we study an enhancement of foregoing scheme by offering additional *reflection* diversity gain. In this scheme, the IRS is configured using random and independent reflection coefficients during multiple consecutive pilot symbols transmitted at the beginning of each time slot. Note that, in this scheme, there is a one-to-one mapping between the pilot symbol index and the phase configuration used at the IRS. Hence, the effective channel between the BS and the  $k$ th user during the  $q$ th pilot transmission in a given time slot, denoted by  $h_{k,q}$ , is different for each of the pilot symbols because the phase configuration of the IRS is different for each value of  $q$ .

1) *Channel Model*: We model the effective downlink channel  $h_{k,q}$  using (4), with the phase configuration  $\Theta$  replaced with  $\Theta_q$  for the  $q$ th pilot interval.

2) *Scheme for IRS-Enhanced Multi-user Diversity Aided with Reflection Diversity*: Inspired by the fast switching time of IRS phase configurations [30], [31] compared to the time slot of transmission (e.g., 10 ms frame duration in 5G NR [32]), we can obtain additional reflection diversity on top of the multi-user diversity by configuring the IRS with several random and independent reflection coefficients (phase configurations) during the pilot symbols transmitted at the beginning of each time slot. Every user chooses the best configuration among all the IRS phase configurations in every

<sup>4</sup>Note that the rate obtainable in an IRS assisted OC system always increases with  $N$ . However, if  $N$  is increased keeping  $K$  fixed, the gap between the rate achieved by OC and the rate achievable under the beamforming configuration with fair resource allocation across users also increases, because the probability that no user is close to beamforming configuration increases. In fact, for a fixed  $K$ , the average rate in a randomly configured IRS grows as  $\mathcal{O}(\log N)$  (see (11)), whereas, in the beamforming configuration, it grows as  $\mathcal{O}(\log N^2)$  (see (5)).

time slot, computes its PF metric, and the best user feeds back the corresponding pilot symbol index and SNR to the BS.<sup>5</sup> The BS then programs the IRS with the phase configuration received from the user selected for transmission, for the rest of the slot.

Let  $Q$  be the number of randomly chosen IRS phase configurations within a time slot, which is the same as the number of pilot transmissions. In the rest of this section, for analytical tractability, and similar to [33], we consider the path loss coefficients to be equal across all links and users:  $\beta_{r,k} \approx \beta_{d,k} = \beta$ .<sup>6</sup> The immediate consequence of this is that the effective channels,  $h_{k,q}$ , are i.i.d. across users and pilot symbols for  $Q \ll K$ . Also, note that, as  $Q$  increases, the time remaining for data transmission in each frame decreases. Thus, the average throughput of a system adopting this scheme is

$$R^{(K,Q)} = (1 - \zeta Q) \mathbb{E} \left[ \log_2 \left( 1 + \max_{\substack{q \in [Q], \\ k \in [K]}} \frac{P|h_{k,q}|^2}{\sigma^2} \right) \right], \quad (10)$$

where  $(1 - \zeta Q)$  is the pre-log factor accounting for the loss in the throughput due to transmitting  $Q$  pilot symbols in each slot,  $\zeta$  is the fraction of the time slot expended in a single pilot transmission, and the expectation is taken with respect to the random IRS phase configurations. Note that we account for the  $(1 - \zeta Q)$  factor only in this subsection, since multiple pilot symbols are used. In rest of the paper, since only a single pilot transmission occurs, we ignore its effect on the throughput. The following theorem analytically characterizes the scaling of the average system throughput of IRS enhanced multi-user diversity aided with reflection diversity as a function of the system parameters.

**Theorem 2.** Consider an  $N$ -element IRS aided system with  $K$  users and  $Q$  pilot transmissions, as described above. If the channels across all users are i.i.d. such that  $h_{k,q} \sim \mathcal{CN}(0, \beta(N+1))$ , the average system throughput scales as

$$\lim_{K \rightarrow \infty} \left( R^{(K,Q)} - (1 - \zeta Q) \times \log_2 \left( 1 + \frac{\beta P}{\sigma^2} (N+1) \ln(QK) \right) \right) = 0. \quad (11)$$

*Proof.* See Appendix A. ■

Another view of the logarithmic scaling in (11) is as follows: When we use  $Q$  pilots and if  $K$  is large enough (with  $Q \ll K$ ), essentially, each of the  $Q$  phase configurations will typically be *near-optimal* for a distinct user. Hence, this scheme allows us to pick the best among these  $Q$  users, which in turn offers a better throughput than the single-pilot transmission. Thus, if  $\zeta$  in (11) is negligible, we see that the throughput depends on  $Q$  and  $K$  only through their product  $QK$ .

In (11), the pre-log factor decreases with  $Q$ , while the logarithmic factor increases with  $Q$ . Therefore, the exists a  $Q$

<sup>5</sup>In slowly varying channels, one can maintain the history of the phase configurations used in the previous time slots and the corresponding SNRs reported by the users, and avoid multiple pilot transmissions in each slot.

<sup>6</sup>The first approximation is realistic as long as IRS path is not much longer than the non-IRS path. Also, due to the second equality, the PF scheduler boils down to the max-rate scheduler [25].

for which (11) is maximized. The following lemma provides the optimal  $Q$  as the solution of an implicit equation, which can be solved using fixed-point iteration methods.

**Lemma 2.** *The number of pilots  $Q$  that maximizes  $R^{(K,Q)}$  in (11) for a given  $K$  and  $N$ , denoted by  $\hat{Q}$ , satisfies the fixed point equation*

$$\log_2(QK) = \frac{1}{\beta(N+1)} e^{W(\zeta^{-1}Q^{-1}-1)}, \quad (12)$$

where  $W(\cdot)$  is the Lambert W function. Then, the optimal integer valued  $Q$  is,

$$Q^* = \arg \max_{\lceil \hat{Q} \rceil, \lfloor \hat{Q} \rfloor} R^{(K,Q)}. \quad (13)$$

*Proof.* Differentiating the limiting value of  $R^{(K,Q)}$  in (11) w.r.t  $Q$ , equating it to zero, and recalling that the solution for  $x$  in  $xe^x = y$  is given by the Lambert W function,  $x = W(y)$ , we obtain (12). The result in (13) follows because the limiting value of  $R^{(K,Q)}$  in (11) is a unimodal function of  $Q$ . ■

**Remark 2.** *The feedback requirement in this scheme is slightly higher than the previous scheme. In addition to feeding back the best overall SNR, each user also sends an additional  $\log_2 Q$  bits to indicate the index of the IRS phase configuration that yielded this best SNR at the user. Furthermore, after scheduling the user by the BS, the BS has to inform the IRS to configure to the phase configuration that gave the best SNR to the scheduled user. However, this additional signalling is still substantially lower than the signalling required by conventional IRS phase optimization schemes.*

**Remark 3.** *Continuing with Remark 1, in order to ensure that with probability at least  $P_{\text{succ}}$ , there is a user for which the IRS configuration used in one of the  $Q$  pilots is within an  $\epsilon$  ball of its optimal beamforming configuration, we need*

$$K \geq \frac{1}{Q} (-\log(1 - P_{\text{succ}})) (\pi/\epsilon)^N,$$

when  $\epsilon/\pi \ll 1$ . Thus, employing  $Q$  random phase configurations at the IRS during the pilot transmissions is equivalent to having  $KQ$  users in the system. Hence, one can achieve a performance close to that achieved by the optimal beamforming configuration at the IRS with fewer users compared to the scheme in Sec. III-A2. Further, if the channel remains constant for, say,  $S$  slots, the feedback obtained from the users in the previous  $S$  slots can be used, so that  $Q$  can be replaced with  $SQ$  in the above bound, thereby further reducing the number of users that need to be in the system. However, this requires a slightly higher overhead in communicating with the IRS: the BS needs to send  $\log_2(SQ)$  bits to configure the IRS in each slot instead of  $\log_2(Q)$  bits.

### C. IRS Channel Model Aware Multi-user Diversity

In the preceding section, a method to improve the performance of the basic scheme in Sec. III-A was proposed by introducing multiple pilot transmissions. However, as we will see from Sec. V, for both the schemes, the gap between the optimal rate and opportunistic rate increases with the number

of IRS elements, especially in the large user regime. We now describe a method to further overcome this limitation by accounting for the channel structure in IRS aided systems, namely, that the IRS is deployed such that the BS-IRS and IRS-user channels exhibit strong LoS paths. On the other hand, the direct link between the BS and user may be non-LoS and experience high path loss/shadowing effects. Thus, in this section, we ignore the contribution of the direct link between the BS and the user, as in [34].

1) *Channel Model:* We represent  $\mathbf{h}_1$  and  $\mathbf{h}_{2,k}$  as LoS channels using array steering vectors. Considering an  $N$ -element uniform linear array (ULA) based IRS, the channels can be modeled as [34]

$$\mathbf{h}_1 = \left[ 1, e^{-j\frac{2\pi d}{\lambda} \sin(\theta_A)}, e^{-j\frac{4\pi d}{\lambda} \sin(\theta_A)}, \dots, e^{-j\frac{2\pi(N-1)d}{\lambda} \sin(\theta_A)} \right]^T, \quad (14)$$

and

$$\mathbf{h}_{2,k} = h'_k \left[ 1, e^{-j\frac{2\pi d}{\lambda} \sin(\theta_{D,k})}, e^{-j\frac{4\pi d}{\lambda} \sin(\theta_{D,k})}, \dots, e^{-j\frac{2\pi(N-1)d}{\lambda} \sin(\theta_{D,k})} \right]^T, \quad (15)$$

where  $\theta_A$  and  $\theta_{D,k}$  are the direction of arrival (DoA) and direction of departure (DoD) of the  $k$ th user at the IRS,  $d$  and  $\lambda$  are the inter-IRS element distance and signal wavelength, and  $h'_k$  is the Rayleigh distributed channel for the  $k$ th user. The other parameters are as in Sec. III-A1 except for the absence of the non-IRS path. For the analysis, the total path loss is considered to equal  $\beta$  for all users as in [33].

2) *Scheme for IRS Channel Model Aware Multi-user Diversity:* Since the locations of the IRS and BS are fixed, and owing to the strong LoS path between the BS and IRS, it is realistic to consider that the channel  $\mathbf{h}_1$  remains constant for relatively long time intervals [35]. Hence, we assume that the knowledge of  $\mathbf{h}_1$  is available at the IRS. For example, we can perform a system calibration to estimate the channel  $\mathbf{h}_1$  offline.<sup>7</sup> Further, in slow fading scenarios, the DoD statistics of all the users (at the IRS) do not change significantly over multiple time slots. Thus, by means of this historic information, the BS could potentially initialize the IRS with the range of DoDs to all the users. The IRS subsequently draws the phase angles from a distribution that depends on the DoD statistics. To this end, we first derive a distribution from which IRS phase angles can be randomly drawn. With  $\theta'_k \triangleq \frac{2\pi d}{\lambda}(\sin(\theta_A) + \sin(\theta_{D,k}))$ , the channel seen by user  $k$  for the IRS configuration  $\Theta$  is given by

$$h_k = \sqrt{\beta} \mathbf{h}_{2,k}^T \Theta \mathbf{h}_1 \quad (16)$$

$$= \sqrt{\beta} h'_k \sum_{n=1}^N e^{-j((n-1)\theta'_k) + j\theta_n}.$$

Thus, the channel gain  $|h_k|$  is maximized iff  $\theta_i = \frac{2\pi(i-1)d}{\lambda}(\sin(\theta_A) + \sin(\theta_{D,k}))$  for all  $i$ , due to the Cauchy-

<sup>7</sup>One approach to accomplish this is illustrated in [21]. The authors rely on an active receiver near the IRS, whose channel to the BS is similar to that of the BS-IRS channel. Then, estimating the channel between the BS and this active receiver can help in estimating  $\mathbf{h}_1$ .

Schwarz inequality and hence denotes the beamforming configuration of the IRS.

Let the DoA at the IRS from the BS be  $\theta_A$  and let the DoDs at the IRS to the users be confined in the range  $[\phi_0, \phi_1]$ . Then, in every time slot, the  $i$ th element of the IRS randomly chooses its phase configuration  $\theta_i$  as follows:

$$\theta_i = \frac{2\pi(i-1)d}{\lambda}(\sin(\theta_A) + \sin(\phi)), \quad (17)$$

where  $\phi \sim \mathcal{U}[\phi_0, \phi_1]$ . The rest of the scheme proceeds as in Sec. III-A2, with the BS scheduling the user with the highest PF metric for data transmission in the current slot.

To investigate the performance of this scheme, first, using (16), it is clear that

$$|h_k|^2 = \beta \left| \sum_{n=1}^N e^{-j((n-1)\theta'_k - \theta_n)} \right|^2 \cdot |h'_k|^2. \quad (18)$$

The maximum value of the first term in (18) is  $\beta N^2$  which is achieved by the beamforming configuration. Thus, when  $K$  is large, for every  $\eta \in (0, 1)$ , there exists a  $\delta > 0$  such that, for a subset of  $\eta K$  users, almost surely, we have [25]

$$\beta \left| \sum_{n=1}^N e^{-j((n-1)\theta'_k - \theta_n)} \right|^2 > \beta N^2 - \delta. \quad (19)$$

On the other hand, the second term in (18) denotes the square of the channel gains, which are i.i.d. across users. We characterize the behavior of this term using extreme value theory (EVT). In particular, using Lemma 3, it can be shown that  $\max_k |h'_k|^2$  grows as  $\ln K$ . Hence, among the  $\eta K$  users, the maximum of  $|h_k|^2$  grows with  $K$  atleast as fast as

$$(\beta N^2 - \delta) \ln(\eta K) = (\beta N^2 - \delta) \ln(K) + \mathcal{O}(1), \quad (20)$$

as  $K \rightarrow \infty$ . Clearly, the case with  $\delta = 0$ , which happens when at least one user is in beamforming configuration, serves as an upper bound on the rate of growth of the  $|h_k|^2$  in (20). As a consequence, we have the following proposition.

**Proposition 1.** *For the IRS channel model aware multi-user diversity scheme, the average system throughput scales as*

$$\lim_{K \rightarrow \infty} \left( R^{(K)} - \mathcal{O} \left( \log_2 \left( 1 + \frac{\beta P}{\sigma^2} N^2 \ln K \right) \right) \right) = 0. \quad (21)$$

The term  $N^2$  in (21) shows that this scheme attains the maximum possible array gain from the IRS by exploiting the presence of strong LoS paths, while the  $\log K$  term is due to multiuser diversity. This scheme even outperforms the scheme where optimization methods are used in IRS aided systems without multiuser diversity (for e.g., see (5)).

**Remark 4.** *Note that, in (17), the value of  $\phi$  is fixed over all the IRS elements, unlike the completely random scheme in Sec. III-A. So, the degrees of freedom in randomness is fixed at 1, i.e., it does not scale with  $N$ . Thus, along the lines of Remark 1, we have that,  $\Pr(\mathcal{E}) = 1 - (1 - (\frac{\epsilon}{\pi}))^K$ . As a consequence, the  $K$  required for near-optimal beamforming does not grow with  $N$ . Hence, the rate of convergence of opportunistic rate to the beamforming based rate is much*

faster compared to scheme in Sec. III-A. These observations are illustrated in Figs. 6 and 7 later in the sequel.

#### IV. SINGLE IRS ASSISTED OPPORTUNISTIC USER SCHEDULING FOR WIDEBAND CHANNELS

In this section, we investigate IRS assisted OC over an  $L$  tap wideband channel. We consider a multiuser OFDM system where all users in the system are served over a given total bandwidth. Since the IRS operates over the entire bandwidth (i.e., it is not possible to apply different phase configurations for different sub-bands),<sup>8</sup> we first analyze the performance of an IRS assisted OFDM system where all the subcarriers are allocated to a single user who has the best channel condition collectively among the subcarriers. In the second scheme, we configure the OFDM based multiple access (OFDMA) and study the performance improvement offered by the multiplexing gain in addition to multi-user diversity. We refer the former scheme as single-user OFDM (SU-OFDM) and latter scheme as OFDMA. As before, for the analysis, we assume that all users experience similar large scale propagation effects with path loss coefficient  $\beta$ , and hence we model the channels across the users in an i.i.d. fashion.

##### A. IRS Enhanced Multi-user Diversity in a Single-user OFDM (SU-OFDM) System

*1) Channel Model:* Consider a time domain channel seen by the  $k$ th user in an  $N$ -element IRS setting. Let  $\mathbf{h}_{d,k} \in \mathbb{C}^{L \times 1}$  be the  $L$ -tap channel between the BS and user  $k$  through the direct (non-IRS) path. Let  $\mathbf{H}_{2,k} \in \mathbb{C}^{N \times L}$  denote the  $L$ -tap channel between IRS and user  $k$  across all IRS elements. Note that, without loss of generality, we assume that the number of taps in the direct channel and the IRS-user channel to be the same. This can be done by letting  $L$  denote the maximum of the number of taps in the two channels. Since the channel between the BS and IRS is typically LoS, it can be modeled as a single-tap channel between the BS and each of the  $N$  elements of the IRS, denoted by  $\mathbf{h}_1 \in \mathbb{C}^{N \times 1}$  (see [12].) Furthermore, due to the strong LoS component,  $\mathbf{h}_1$  can be modelled as an array steering response vector when the IRS is configured as a ULA (see (14)). We assume that channels between the IRS and the users across all the  $L$  taps are independent of each other [5], [35]. The exact statistics of the channels are provided below. The composite channel of user  $k$  can then be compactly written as

$$\mathbf{h}_k = \mathbf{h}_{d,k} + \mathbf{H}_{2,k}^T \Theta \mathbf{h}_1 \in \mathbb{C}^{L \times 1}. \quad (22)$$

In this work, we use an exponentially decaying power delay profile (PDP) in the lag domain. Let  $\check{h}_{k,l,n} \triangleq h_{1,n} h_{2,k,l,n}$  denote the gain of the  $l$ th tap of the fading channel between the BS and the  $k$ th user through the  $n$ th IRS element. Then, the PDP of the link is given by

$$a_l \triangleq \mathbb{E}[|\check{h}_{k,l,n}|^2] = ce^{-\nu l/L}, \quad \forall k \in [K], n \in [N], \quad (23)$$

<sup>8</sup>Note that, in this paper, we assume that the IRS elements are not frequency selective, similar to past work in the area [11], [36]. In fact, by appropriately designing the tuning parameters of the IRS circuit elements, it is possible to achieve non-frequency selectivity of the IRS elements even in wideband systems [37].

where  $c$  is chosen such that  $\sum_l \mathbb{E}[|\check{h}_{k,l,n}|^2] = 1$ , and  $\nu$  captures the decay rate of the channel tap power with  $l$ . Hence, we have,  $\|\mathbf{a}\|_1 = 1$ , where  $\mathbf{a} \triangleq [a_1, a_2, \dots, a_L]^T$  represents the power in each of the  $L$  taps. Therefore, the  $l$ th component of the channel in (22) can be written as  $h_{k,l} = h_{d,k,l} + \sum_{i=1}^N e^{j\theta_i} \check{h}_{k,l,i}$ . If  $h_{d,k,l}, h_{2,k,l,i} \sim \mathcal{CN}(0, a_l)$  across the IRS elements and since  $|h_{1,n}|^2 = 1$  for all  $n \in [N]$ , it is easy to show that  $h_{k,l} \sim \mathcal{CN}(0, (N+1)a_l)$  and independent across the users and  $L$  taps. Equivalently, in the OFDM system with  $M$  subcarriers, if we let  $\tilde{\mathbf{h}}_k \in \mathbb{C}^{M \times 1}$  denote the frequency-domain channel vector for user  $k$ , we have  $\tilde{\mathbf{h}}_k = \mathbf{F}_{M,L} \mathbf{h}_k$  where  $\mathbf{F}_{M,L}$  is the matrix containing the first  $L$  columns of the  $M \times M$  DFT matrix.<sup>9</sup> Thus, the channel at subcarrier  $m$  for user  $k$  follows  $\tilde{h}_k[m] \sim \mathcal{CN}(0, N+1)$ , and we also have the Parseval's relation  $\mathbb{E}[\|\tilde{\mathbf{h}}_k\|_2^2] = M \mathbb{E}[\|\mathbf{h}_k\|_2^2]$ .

2) *Scheme for IRS-Enhanced Multi-user Diversity in SU-OFDM Systems:* As before, we randomly set the phase configuration at the IRS in every time slot. The BS then applies equal power on all the subcarriers and broadcasts pilot symbols to all the users. In this section, for simplicity and analytical tractability, we assume that the BS uses equal power allocation across subcarriers during data transmission also; note that this is near-optimal in the high SNR regime. The users estimate the channels and compute the sum rate obtainable by them across all the subcarriers, and compute their respective PF metrics. The user with the highest PF metric sends its identity back to the BS, and is scheduled for transmission using all the subcarriers by the BS. Note that, with a slightly higher feedback overhead, the scheme easily extends to the case where optimal water-filling power allocation is used by the BS. Here, after estimating the channels across the subcarriers, the user computes the sum rate achievable by it with water-filling power allocation, and uses this to compute its PF metric. In this case, instead of feeding back a packet containing the user identity and the SNR, the user with the highest PF metric will also need to include the power allocation vector, which is of size  $\approx 4M$  bits (assuming 16-levels of power control in each subcarrier.)

Under equal power allocation, in a  $K$  user system, the maximum average sum rate obtainable across subcarriers with a total power constraint  $P$  and noise variance  $\sigma^2$  is

$$R_{\text{SU-OFDM}}^{(K)} = \max_{1 \leq k \leq K} \sum_{m=0}^{M-1} \log_2 \left( 1 + \frac{\beta P}{M\sigma^2} |\tilde{h}_k[m]|^2 \right). \quad (24)$$

In view of (24), we have the following theorem for reasonably large  $L$  (we refer the reader to Remark 6 in Appendix B for a discussion on how large  $L$  needs to be.)

**Theorem 3.** Consider an  $N$ -element IRS assisted SU-OFDM system with  $M$  subcarriers and  $L$  time-domain taps with power delay profile  $\mathbf{a}$  and a total power constraint  $P$  and noise variance  $\sigma^2$ . Then, for large  $L$ , the average sum rate of IRS enhanced multi-user diversity in an SU-OFDM system under equal power allocation,  $R_{\text{SU-OFDM}}^{(K)}$ , scales as

<sup>9</sup>In this paper, we compute the discrete Fourier transform (DFT) as  $X[m] = \sum_{l=0}^{M-1} x[l] e^{-j \frac{2\pi m l}{M}}$  for all  $m \in \{0, 1, \dots, M-1\}$ .

$$\lim_{K \rightarrow \infty} \left( R_{\text{SU-OFDM}}^{(K)} - \mathcal{O} \left( \log_2 \left\{ 1 + \frac{\beta P}{\sigma^2} (N+1) \times \left[ 1 + \|\mathbf{a}\|_2 \Phi^{-1} \left( 1 - \frac{1}{K} \right) \right] \right\} \right) \right) = 0, \quad (25)$$

where  $\Phi^{-1}(\cdot)$  is the inverse of the cumulative distribution function (cdf) of a standard normal random variable. ■

*Proof.* See Appendix B.

In the above result, since the argument of  $\Phi^{-1}(\cdot)$  is close to 1 for large  $K$ , we can use  $\Phi(x) \approx \frac{1}{2} \left( 1 + \sqrt{1 - e^{-\frac{2}{\pi} x^2}} \right)$  [38]. Consequently, from (25), we can explicitly determine the dependence of the sum rate on  $K$ , as in the following corollary.

**Corollary 1.** For the setup in Theorem 3, we have

$$\lim_{K \rightarrow \infty} \left( R_{\text{SU-OFDM}}^{(K)} - \mathcal{O} \left( \log_2 \left\{ 1 + \frac{\beta P}{\sigma^2} (N+1) \times \left[ 1 + \|\mathbf{a}\|_2 \sqrt{\frac{\pi}{2} \ln K} \right] \right\} \right) \right) \approx 0. \quad (26)$$

Comparing the SU-OFDM performance given by the above equation with the performance in narrowband channels (see (11), with  $Q = 1$ ), the main difference in the multi-carrier case is the presence of  $\|\mathbf{a}\|_2$  and the dependence on the number of users as  $\sqrt{\ln K}$  instead of  $\ln K$ . The  $\sqrt{\ln K}$  dependence is a consequence of the upper-bounding technique used to obtain (26); and apart from the  $\|\mathbf{a}\|_2$  factor, the performances are similar in the two cases. This will be illustrated in Sec. V.

### B. IRS Enhanced Multi-user Diversity in OFDMA Systems

We now consider an OFDMA system, where, instead of allotting all the subcarriers to one of the users, each subcarrier is allotted to a single, possibly different user. On the other hand, a given user can be allotted one or more subcarriers. We consider the same channel model as in Sec. IV-A1.

1) *Scheme for IRS-Enhanced Multi-user Diversity in OFDMA Systems:* The scheme is similar to the single-user OFDM system in Sec. IV-A, except that the user scheduling is done on a per subcarrier basis instead of allotting all the subcarriers to the user with the best sum rate across subcarriers. Recall that the channel coefficient of the  $m$ th subcarrier of user  $k$  is denoted by  $\tilde{h}_k[m]$ . Then, the average sum rate under equal power allocation in the IRS enhanced OFDMA based multi-user diversity scheme is given by

$$R_{\text{OFDMA}}^{(K)} = \sum_{m=0}^{M-1} \log_2 \left\{ 1 + \frac{\beta P}{M\sigma^2} \max_{1 \leq k \leq K} |\tilde{h}_k[m]|^2 \right\}. \quad (27)$$

Thus, we have the following theorem that characterizes the average sum rate of an OFDMA system.

**Theorem 4.** Consider an  $N$ -element IRS assisted OFDMA system with  $M$  subcarriers, a total power constraint  $P$ , and noise variance  $\sigma^2$ . Then, the average sum rate exploiting multi-user diversity under equal power allocation,  $R_{\text{OFDMA}}^{(K)}$ , scales as

$$\lim_{K \rightarrow \infty} \left\{ R_{\text{OFDMA}}^{(K)} - M \log_2 \left( 1 + \frac{\beta P}{M\sigma^2} (N+1) \ln K \right) \right\} = 0. \quad (28)$$

*Proof.* The key step is to characterize the random variable  $\max_{1 \leq k \leq K} |\tilde{h}_k[m]|^2$  for large  $K$ . Since  $|\tilde{h}_k[m]|^2 \stackrel{\text{i.i.d.}}{\sim} \exp(1/(N+1))$ , we can apply Lemma 3 to obtain the scaling law in (28) in the same way as derived in Appendix A. ■

**Remark 5.** The IRS assisted OFDMA scheme outperforms the SU-OFDM scheme due to two reasons: 1) Since there are  $M$  parallel channels in the OFDMA scheme, and this offers additional selection/frequency diversity gain over an SU-OFDM system. 2) While a given user may see different channel coefficients on different subcarriers, the IRS configuration is common across all subcarriers. Thus, even in the asymptotic number of users, it is not possible for any user to be in beamforming configuration on all the subcarriers in an SU-OFDM scheme. On the other hand, in the OFDMA scheme, since the setup boils down to the availability of  $M$  parallel channels, and when  $K$  is large, it is possible for the IRS to be close to the beamforming configuration with high probability on all subcarriers, by scheduling different users on the different subcarriers. However, the feedback overhead in the OFDMA scheme is  $M$  times that of SU-OFDM, since the BS needs to find the best user on each of the  $M$  subcarriers. Note that, with OFDMA, one can still use a low feedback overhead timer- or splitting-based scheme [28], [29] for identifying the best user to schedule for data transmission, but on a subcarrier-by-subcarrier basis.

## V. NUMERICAL RESULTS

In this section, we validate the analytical results derived as well as quantify the relative performance of the different schemes proposed in the previous sections, through Monte Carlo simulations. A single antenna BS is located at  $(0, 0)$  (in metres), the IRS is at  $(0, 250)$  and single antenna users are uniformly distributed in the rectangular region with diagonally opposite corners  $(100, 500)$  and  $(500, 1000)$ . The path losses are computed as  $\beta = 1/d^\alpha$  where  $d$  is the distance and  $\alpha$  is the path loss exponent. We use  $\alpha = 2, 2.8$  and  $3.6$  in the BS-IRS, IRS-user and BS-user (direct) links, respectively [5]. Further, we consider a BS transmitting with power  $P = -10$  dBm and noise variance at the receiver  $\sigma^2 = -117.8$  dBm, corresponding to a signal bandwidth of 400 kHz at a temperature of 300 K. Then, in the absence of the IRS, a user at the point closest to the BS experiences an average SNR of about 10.3 dB, while the farthest user experiences an average SNR of  $-1.9$  dB. The fading channels are randomly generated as per the distributions discussed in the previous sections.

We first evaluate the performance of the scheme described in Sec. III-A. In Fig. 3, we plot the average throughput offered by a randomly configured IRS-assisted OC scheme operated using a proportional fair scheduler with  $T_c = 5000$ . We compare the performance of the OC scheme against that of the beamforming-optimal scheme, given by (7). The throughput of the OC system improves with the number of IRS elements and users in the system. On the other hand, the gap between the throughput of the OC scheme and that of the optimally configured IRS based scheme also increases with the number of IRS elements, in line with our discussion in Remark 1. We also see that the IRS assisted system significantly outperforms

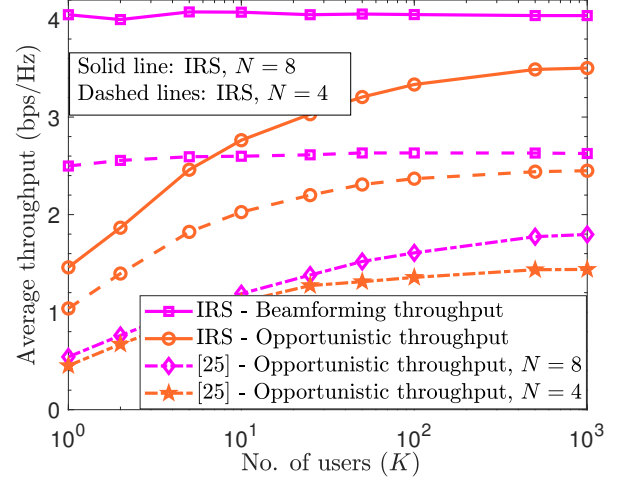


Fig. 3: Average throughput vs. the number of users compared with the opportunistic scheme in [25].

opportunistic scheduling in the absence of the IRS [25], when the BS is equipped with  $N$  antennas (i.e., the same as the number of IRS elements used).<sup>10</sup> This is because the BS is constrained by a total radiated power. Hence, increasing the number of antennas reduces the transmit power per antenna, and results in a throughput that improves only marginally with the number of antennas at the BS. On the other hand, since the IRS uses passive reflective elements, the total received power at the user increases quadratically with the number of IRS elements under the optimal beamforming configuration (see, e.g., Proposition 1 or [7]).

Next, in Figs. 4 and 5, we evaluate the scheme in Sec. III-B. In this experiment, we use  $\zeta = 0.01$  in (11). Hence, the rate goes to zero when  $Q = 100$ , since no symbols are left for data transmission. In Fig. 4, we plot the throughput as a function of  $Q$ , the number of pilot transmissions. The optimal  $Q^*$  that yields the best trade-off between the pilot overhead and reflection diversity gain, given by (13), agrees with the integer  $Q$  at which the throughput achieves its maximum. In Fig. 5, we compare the performance obtained using  $Q = 1$  (as in Fig. 3) against that obtained by using  $Q = Q^*$  pilot transmissions. The figure clearly shows the additional gain due to the reflection diversity, particularly when the number of users is small. The gain is marginal when  $K$  is large, partly because the throughput depends weakly on  $Q$  since it scales as  $\log(\ln(QK))$ , and partly because  $Q^*$  itself reduces with  $K$ . On the same figure, we also plot the performance of the IRS assisted opportunistic system under equal path loss across users, and see that the simulations match well with the theoretical result in Theorem 2.

In Fig. 6, we study the performance of the channel model aware OC scheme as in Sec. III-C and the IRS draws phase angles randomly as per (17), where  $\phi_0 = -40^\circ$ ,  $\phi_1 = 40^\circ$  and  $\theta_A = 20^\circ$ . We also use the uniform distribution to draw the phase angles at all the IRS elements independently, and

<sup>10</sup>The BS uses weights  $\alpha_n(t)$  and phase  $\theta_n(t)$  at the  $n$ th antenna at time  $t$ , leading to  $h_k(t) = \sum_{n=1}^N \sqrt{\alpha_n(t)} e^{j\theta_n(t)} h_{nk}(t)$  as the effective channel gain. At each  $t$ ,  $\alpha_n(t)$  and  $\theta_n(t)$  are set randomly.

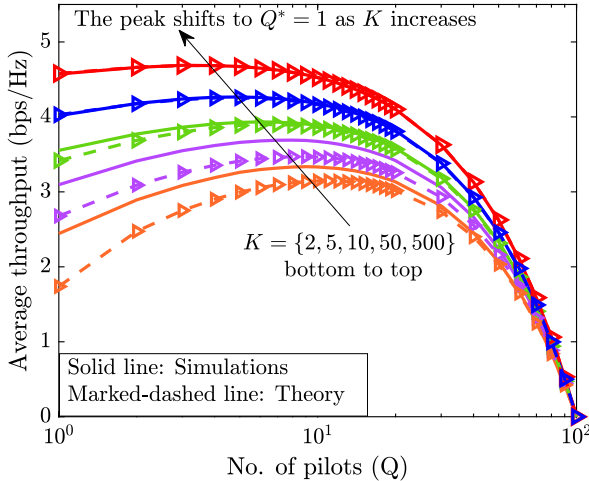


Fig. 4: Average throughput as a function of the number of pilot transmissions, for  $N = 8$ .

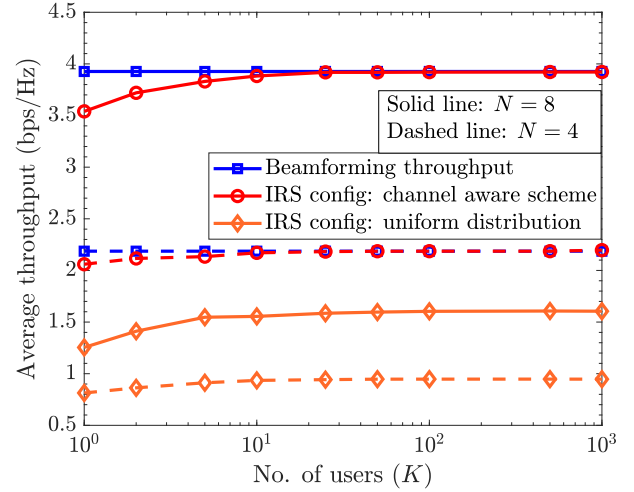


Fig. 6: Average throughput as a function of the number of users, for channel model aware scheme.

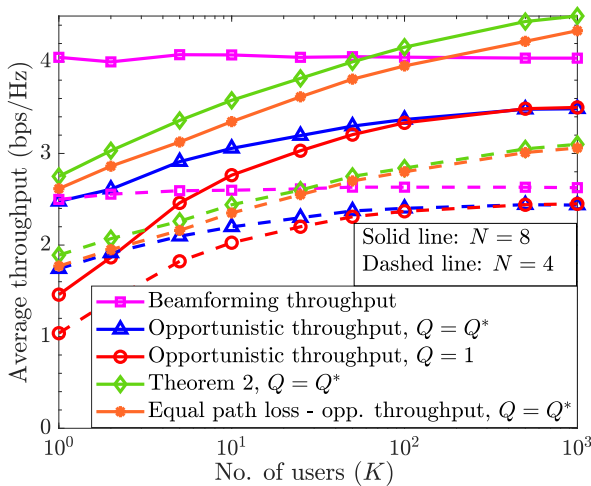


Fig. 5: Average throughput as a function of the number of users, with  $Q^*$  pilot transmissions.

show its performance in the same figure. We see that the performance of the OC system improves dramatically when channel model and DoD statistics at the IRS are used in selecting the phase configurations.

Next, in Fig. 7, we investigate the performance gap between the randomly configured IRS based OC and the rate obtained from the beamforming configuration, as a function of number of IRS elements with and without the knowledge of DoD statistics at the IRS. The different curves correspond to the system having varying number of users. We see that, for a given number of users, the performance of the system with the IRS phase angles drawn exploiting the knowledge of the DoD statistics is very close to the performance of an optimized IRS even if the number of IRS elements is as large as 1024. Furthermore, in this regime, even when the number of users in the system is as small as 50, the OC performance is still close to the coherent beamforming rate. On the other hand, the performance of an IRS assisted OC scheme with the phase angles drawn independently from the uniform distribution

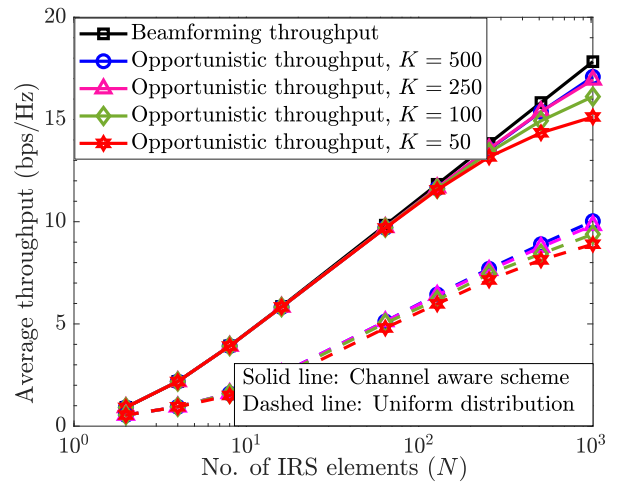


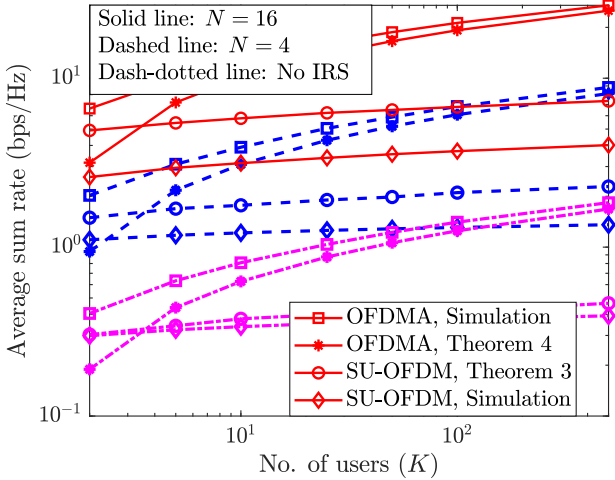
Fig. 7: Average throughput as a function of the number of IRS elements, for different number of users.

becomes increasing worse relative to the beamforming rate as the number of IRS elements increases. Moreover, the effect of multi-user diversity is hardly evident in the latter case, when the number of IRS elements is large. In a nutshell, for a given number of users, the channel model aware scheme offers two benefits: 1) The rate of the OC system remains close to the optimal beamforming rate even with a large number of IRS elements; 2) The effect of multi-user diversity is well captured, even with a small number of users.

As the last experiment in this section, we consider the performance of IRS aided OC over wideband channels as discussed in Sec. IV. We fix the number of time domain channel taps,  $L = 25$  [39] with  $\nu = 1$  in (23), and perform communication through an OFDM system with  $M = 64$  subcarriers with subcarrier spacing is set to 60 kHz (this corresponds to a numerology of 2 in 5G NR.) As a result, the total system bandwidth is 3.84 MHz which corresponds to a total noise variance  $\sigma^2 = -107.98$  dBm at 300 K. We choose a total power budget  $P = 1$  dBm at the BS and as

TABLE I: Excess kurtosis  $\kappa$  as a function of the number of taps.

$L$	1	2	5	10	20	25	50	100
$\kappa$	5.96	3.52	1.5	0.76	0.35	0.28	0.13	0.07

Fig. 8: Average sum rate as a function of number of users, for an OFDM based communication system with  $M = 64$  subcarriers.

a consequence, the nearest user experiences an average per subcarrier SNR of 11 dB and the farthest user  $-1.2$  dB, respectively. The channels are generated in an i.i.d. fashion across the users by setting the path loss coefficient to be equal for all users, such that the average SNR is 4.3 dB, and the BS power is allotted divided across all the subcarriers. Before we look at the numerical performance of the schemes, we first ascertain the applicability of analytical rate scaling law in (25) for the choice of  $L = 25$  at  $\nu = 1$  in SU-OFDM systems. To characterize the Gaussianity of the sum-term in the left hand side of (37), we compute its excess kurtosis, which measures how close a given distribution is to the Gaussian distribution [40]. The excess kurtosis,  $\kappa$ , of a random variable  $X$  with mean  $\mu$  is defined as

$$\kappa = \frac{\mathbb{E}[|X - \mu|^4]}{(\mathbb{E}[|X - \mu|^2])^2} - 3. \quad (29)$$

For a Gaussian random variable,  $\kappa = 0$ . In Table I, we list the excess kurtosis of the  $L$ -sum term in (37) as a function of  $L$ . We see that, for  $L = 25$ , we obtain an excess kurtosis of approximately 0.28, which is within 4% of the distance between a Gaussian and exponential random variable (corresponding to  $L = 1$ ). Thus, it is reasonable to consider that this sum-term is nearly Gaussian distributed, making the scaling law in (25) valid for  $L = 25$ .

We present the OC performance of SU-OFDM and OFDMA in Fig. 8. The throughput offered by the IRS assisted OFDMA is superior to that of SU-OFDM, in line with Remark 5. We also see that the performance of both OFDMA and SU-OFDM increase with  $N$ , in an IRS-assisted system exploiting multi-user diversity. However, while the simulated and theoretical performance of OFDMA match well as  $K$  increases, there is a gap between the two in the case of SU-OFDM. This is partly because the throughput analysis of SU-OFDM is

an upper bound (see (32)), and partly because the channels across the subcarriers become more disparate as the number of IRS elements increases, making the upper bound looser as  $N$  increases. Nonetheless, the plot shows that one can obtain a performance boost by deploying an IRS, even without using complex optimization algorithms, by merely obtaining multi-user diversity gains over randomly configured IRSs.

## VI. CONCLUSIONS

In this paper, we presented several opportunistic schemes in a single IRS aided setting for exploiting and enhancing the multi-user diversity gains, both in narrowband and wideband channels. The schemes completely avoid the need for CSI estimation and computationally expensive phase optimization, and require little or no communication from the BS to IRS. First, we saw that, in narrowband channels, a basic multi-user diversity scheme using a randomly configured IRS provides a performance boost over conventional systems as the number of users,  $K$ , gets large. In order to improve the rate of convergence of the opportunistic rate to the coherent rate (in terms of the number of users), we presented two alternative approaches: one where we obtained additional reflection diversity, and the other where we exploited the channel structure in IRS assisted systems. Both these schemes improve the rate of convergence of the throughput from the OC schemes with the number of users. In particular, exploiting the channel structure allows us to significantly increase the number of IRS elements (and therefore the throughput) without requiring an exponentially larger number of users to achieve significant multi-user diversity gains. Finally, we considered IRS aided OC over a wideband channel in an OFDM system, and analyzed the performance of two different schemes, namely, SU-OFDM and OFDMA. Overall, IRS assisted OC schemes offer significant performance improvement over conventional schemes, while incurring very low system overheads. A potential direction for future work is to extend the setting to multiuser MIMO-OFDM systems, and develop OC schemes in an IRS-aided framework.

## APPENDIX A PROOF OF THE THEOREM 2

The proof of the theorem uses the following lemma on the extreme values of i.i.d. random variables.

**Lemma 3.** ([25]). *Let  $z_1, \dots, z_K$  be i.i.d. random variables with a common cumulative distribution function (cdf)  $F(\cdot)$  and probability density function (pdf)  $f(\cdot)$  that satisfy  $F(z) < 1$  and is twice differentiable for all  $z$ . Let the corresponding hazard function,  $\Omega(z) \triangleq \left[ \frac{f(z)}{1-F(z)} \right]$  be such that*

$$\lim_{z \rightarrow \psi} \frac{1}{\Omega(z)} = c > 0, \quad (30)$$

for  $\psi \triangleq \sup\{z : F(z) < 1\}$  and some constant  $c$ . Then,  $\max_{1 \leq k \leq K} z_k - l_K$  converges in distribution to a Gumbel random variable with cdf  $e^{(-e^{-x/c})}$ , where  $F(l_K) = 1 - \frac{1}{K}$ .

In words, the lemma states that, asymptotically, the maximum of  $K$  i.i.d. random variables grows like  $l_K$ . From

Theorem 2, it is clear that,  $|h_{k,q}|^2 \sim \exp\left(\frac{1}{\beta(N+1)}\right)$  for all  $k \in [K]$  and  $q \in [Q]$ . Further, since the phase angles are independently generated at the IRS during each pilot transmission, we have that  $\tilde{h} \triangleq |h_{k,q}|^2$  form a set of  $QK$  i.i.d. exponential random variables with mean  $\beta(N+1)$ . Thus we have the pdf,  $f_{\tilde{h}}(h) = \frac{1}{\beta(N+1)}e^{-\frac{h}{\beta(N+1)}}$  for  $h \geq 0$  and hence the cdf,  $F_{\tilde{h}}(h) = 1 - e^{-\frac{h}{\beta(N+1)}}$  for  $h \geq 0$  and 0 otherwise. Also, here  $\psi = \infty$ . Thus, we have,

$$\lim_{h \rightarrow \infty} \Omega(h) = \lim_{h \rightarrow \infty} \frac{e^{-\frac{h}{\beta(N+1)}}}{\frac{1}{\beta(N+1)}e^{-\frac{h}{\beta(N+1)}}} = \beta(N+1) > 0. \quad (31)$$

Hence, by virtue of the above lemma, we have  $l_{QK} = F^{-1}\left(1 - \frac{1}{QK}\right)$  and solving, we get  $l_{QK} = \beta(N+1) \ln(QK)$  and subsequently applying the lemma to (10), we get the desired result.

## APPENDIX B

### PROOF OF THE THEOREM 3

Using Jensen's inequality, (24) can be upper bounded as

$$R_{\text{SU-OFDM}}^{(K)} \leq \max_{1 \leq k \leq K} \log_2 \left( 1 + \frac{\beta P}{M\sigma^2} \sum_{m=0}^{M-1} |\tilde{h}_k[m]|^2 \right). \quad (32)$$

From Parseval's theorem,  $\sum_{m=0}^{M-1} |\tilde{h}_k[m]|^2 = M \sum_{l=0}^{L-1} |h_{k,l}|^2$ . Using the monotonicity of log and simplifying, we get

$$R_{\text{SU-OFDM}}^{(K)} \leq \log_2 \left( 1 + \frac{\beta P}{\sigma^2} \left\{ \max_{1 \leq k \leq K} \sum_{l=0}^{L-1} |h_{k,l}|^2 \right\} \right). \quad (33)$$

Recall that for a given  $k$ ,  $h_{k,l} \sim \mathcal{CN}(0, (N+1)a_l)$ . Hence, for a given  $k$ ,  $|h_{k,l}|^2 \sim \exp\left(\frac{1}{(N+1)a_l}\right)$  and form a set of independent and non identically distributed random variables across  $L$  taps. We now use the fact that  $L$  is large and invoke the following version of the central limit theorem (CLT) [41]:

**Lemma 4** (Lyapounov's Central Limit Theorem). *Suppose that  $X_1, X_2, \dots, X_n$  form a sequence of independent random variables such that  $\forall i \in [n]$ , define  $\mathbb{E}[X_i] \triangleq \mu_i$ ,  $\sigma_i^2 \triangleq \mathbb{E}[|X_i|^2]$  and  $s_n^2 \triangleq \sum_{i=1}^n \sigma_i^2$ . If for some  $\delta > 0$ ,*

$$\mathcal{L} \triangleq \lim_{n \rightarrow \infty} \sum_{i=1}^n \frac{1}{s_n^{2+\delta}} \mathbb{E}[|X_i - \mu_i|^{2+\delta}] = 0, \quad (34)$$

then

$$\frac{1}{s_n} \sum_{i=1}^n (X_i - \mu_i) \xrightarrow[n \rightarrow \infty]{d} \mathcal{CN}(0, 1), \quad (35)$$

where  $\xrightarrow[n \rightarrow \infty]{d}$  stands for convergence in distribution.

To check whether the random variables  $\{|h_{k,l}|^2\}_l$  satisfy (34), let  $\delta = 1$ . Then  $\mathbb{E}[|X_i - \mu_i|^3] = 2((N+1)a_l)^3$ . Further,  $s_n^2 = \sum_{i=1}^n a_l^2 (N+1)^2$ , hence  $s_n^3 = (\|\mathbf{a}\|_2 (N+1))^3$ . Thus,  $\mathcal{L} = \lim_{n \rightarrow \infty} 2 \frac{\|\mathbf{a}\|_2^3}{\|\mathbf{a}\|_2^2}$ . We can lower and upper bound the ratio in the right hand side as follows:

$$2 \frac{n \min_{i \in [n]} a_i^3}{n^{3/2} \max_{i \in [n]} a_i^3} \leq 2 \frac{\|\mathbf{a}\|_2^3}{\|\mathbf{a}\|_2^2} \leq 2 \frac{n \max_{i \in [n]} a_i^3}{n^{3/2} \min_{i \in [n]} a_i^3}.$$

Hence, when  $n \rightarrow \infty$  and  $\|\mathbf{a}\|_2 < \infty$ , both lower and upper bounds go to zero and thus by the sandwich theorem,  $\mathcal{L} = 0$ . Thus, the given exponential random variables satisfy the condition in the lemma. Therefore, we have,

$$\frac{1}{(N+1)\|\mathbf{a}\|_2} \sum_{l=1}^L (|h_{k,l}|^2 - (N+1)a_l) \xrightarrow[L \rightarrow \infty]{d} \mathcal{CN}(0, 1), \quad (36)$$

which implies

$$\sum_{l=1}^L |h_{k,l}|^2 \xrightarrow[L \rightarrow \infty]{d} (N+1) \{1 + \|\mathbf{a}\|_2 \bar{h}_k\}, \quad (37)$$

where  $\bar{h}_k \sim \mathcal{CN}(0, 1)$ . Thus, (33) can be rewritten as,

$$\begin{aligned} R_{\text{SU-OFDM}}^{(K)} &\leq \log_2 \left( 1 + \frac{\beta P}{\sigma^2} (N+1) \right. \\ &\quad \left. \times \left[ 1 + \|\mathbf{a}\|_2 \left\{ \max_{1 \leq k \leq K} \bar{h}_k \right\} \right] \right). \end{aligned} \quad (38)$$

To characterize the extreme value of  $K$  i.i.d. Gaussian random variables, we note that Lemma 3 cannot be used as (30) is not satisfied by Gaussian random variables. Instead, we use another lemma to characterize the extreme values of i.i.d. Gaussian random variables from [42].

**Lemma 5** (Von Mises' sufficient condition for weak convergence of extreme values). *Let  $X_1, X_2, \dots, X_K$  be i.i.d. random variables and define  $M_K \triangleq \max\{X_1, X_2, \dots, X_K\}$ . Let  $F(x)$  be an absolutely continuous cdf with  $f(x)$  being the corresponding pdf. Let the corresponding hazard function be  $\Omega(x) \triangleq \left[ \frac{f(x)}{1-F(x)} \right]$  and let  $\psi = \sup\{x : F(x) < 1\}$ . If*

$$\lim_{x \rightarrow \psi} \frac{d}{dx} \left( \frac{1}{\Omega(x)} \right) = 0, \quad (39)$$

then,

$$M_K - l_K \xrightarrow[K \rightarrow \infty]{d} G, \quad (40)$$

where  $G$  is a Gumbel random variable with cdf,  $e^{(-e^{-x/c})}$  and  $l_K$  is given by  $F(l_K) = 1 - \frac{1}{K}$  for some constant  $c > 0$ .

As before, the result shows that the extreme value of  $K$  i.i.d. random variables satisfying (39) grows like  $l_K$ , asymptotically. In what follows, we check the applicability of the lemma to  $K$  i.i.d. Gaussian random variables. Clearly,  $\psi = \infty$ . Let  $\Phi(x)$  and  $f(x)$  be the cdf and pdf of a standard complex normal random variable. We then have,

$$\frac{d}{dx} \left( \frac{1 - \Phi(x)}{f(x)} \right) = \frac{(1 - \Phi(x))x}{f(x)} - 1 = \sqrt{2}x \frac{Q(x)}{f(x)} - 1, \quad (41)$$

where  $Q(x)$  is the standard  $Q$  function. But we know that,

$$\frac{1}{\sqrt{2\pi}x} e^{-\frac{x^2}{2}} \left( 1 - \frac{1}{x^2} \right) \leq Q(x) \leq \frac{1}{\sqrt{2\pi}x} e^{-\frac{x^2}{2}}. \quad (42)$$

Using (42) to lower and upper bound (41) and taking the limit  $x$  to  $\infty$  and applying the sandwich theorem, it is straightforward to show that (39) is satisfied by Gaussian random variables. Thus, we have that,  $l_K = \Phi^{-1}\left(1 - \frac{1}{K}\right)$ . Substituting it in (38) yields the desired result in (25).

**Remark 6.** To quantify how large  $L$  should be in order for Theorem 3 to hold, we use the Berry–Esseen theorem [43] which describes the error bound in approximating the normalized sum of random variables to a normal random variable through the CLT. We can show that, the worst case absolute error, i.e.,  $\sup_{x \in \mathbb{R}} |F_n(x) - \Phi(x)| \lesssim C_1 \cdot a_1 / \|\mathbf{a}\|_2$ , where  $F_n(x)$  and  $\Phi(x)$  denote the cdf of the normalized sum-random variable and standard normal random variable, for some constant  $C_1 > 0$ . Thus, for a given  $L$ , this bound becomes tighter when the PDP is slowly decaying, with the power in the dominant tap being comparable to other taps (which occurs when  $\nu$  is small), and in this case, the convergence in CLT occurs faster.

## REFERENCES

- [1] M. Di Renzo, M. Debbah, D.-T. Phan-Huy, A. Zappone, M.-S. Alouini, C. Yuen, V. Sciancalepore, G. C. Alexandropoulos, J. Hoydis, H. Gacanin *et al.*, “Smart radio environments empowered by reconfigurable AI meta-surfaces: An idea whose time has come,” *EURASIP J. Wireless Commun. Netw.*, vol. 2019, no. 1, pp. 1–20, 2019.
- [2] E. Basar, M. Di Renzo, J. De Rosny, M. Debbah, M.-S. Alouini, and R. Zhang, “Wireless communications through reconfigurable intelligent surfaces,” *IEEE Access*, vol. 7, pp. 116 753–116 773, 2019.
- [3] Q. Wu and R. Zhang, “Towards smart and reconfigurable environment: Intelligent reflecting surface aided wireless network,” *IEEE Commun. Mag.*, vol. 58, no. 1, pp. 106–112, 2020.
- [4] E. Björnson, H. Wymeersch, B. Mathiesen, P. Popovski, L. Sanguinetti, and E. de Carvalho, “Reconfigurable intelligent surfaces: A signal processing perspective with wireless applications,” *arXiv preprint arXiv:2102.00742*, 2021.
- [5] Q.-U.-A. Nadeem, A. Chaaban, and M. Debbah, “Opportunistic beamforming using an intelligent reflecting surface without instantaneous CSI,” *IEEE Wireless Commun. Lett.*, vol. 10, no. 1, pp. 146–150, 2021.
- [6] P. Wang, J. Fang, X. Yuan, Z. Chen, and H. Li, “Intelligent reflecting surface-assisted millimeter wave communications: Joint active and passive precoding design,” *IEEE Trans. Veh. Technol.*, vol. 69, no. 12, pp. 14 960–14 973, 2020.
- [7] Q. Wu and R. Zhang, “Intelligent reflecting surface enhanced wireless network: Joint active and passive beamforming design,” in *Proc. IEEE Global Commun. Conf.*, 2018, pp. 1–6.
- [8] C. Huang, A. Zappone, G. C. Alexandropoulos, M. Debbah, and C. Yuen, “Reconfigurable intelligent surfaces for energy efficiency in wireless communication,” *IEEE Trans. Wireless Commun.*, vol. 18, no. 8, pp. 4157–4170, 2019.
- [9] H. Guo, Y.-C. Liang, J. Chen, and E. G. Larsson, “Weighted sum-rate maximization for intelligent reflecting surface enhanced wireless networks,” in *Proc. IEEE Global Commun. Conf.*, 2019, pp. 1–6.
- [10] S. Zhou, W. Xu, K. Wang, M. Di Renzo, and M.-S. Alouini, “Spectral and energy efficiency of IRS-assisted MISO communication with hardware impairments,” *IEEE Wireless Commun. Lett.*, vol. 9, no. 9, pp. 1366–1369, 2020.
- [11] Y. Yang, B. Zheng, S. Zhang, and R. Zhang, “Intelligent reflecting surface meets OFDM: Protocol design and rate maximization,” *IEEE Trans. Commun.*, vol. 68, no. 7, pp. 4522–4535, 2020.
- [12] B. Zheng, C. You, and R. Zhang, “Intelligent reflecting surface assisted multi-user OFDMA: Channel estimation and training design,” *IEEE Trans. Wireless Commun.*, vol. 19, no. 12, pp. 8315–8329, 2020.
- [13] Y. Lin, S. Jin, M. Matthaiou, and X. You, “Channel estimation and user localization for IRS-assisted MIMO-OFDM systems,” *IEEE Trans. Wireless Commun.*, pp. 1–1, 2021.
- [14] H. Li, W. Cai, Y. Liu, M. Li, Q. Liu, and Q. Wu, “Intelligent reflecting surface enhanced wideband MIMO-OFDM communications: From practical model to reflection optimization,” *IEEE Trans. Commun.*, vol. 69, no. 7, pp. 4807–4820, 2021.
- [15] H. Li, R. Liu, M. Liy, Q. Liu, and X. Li, “IRS-enhanced wideband MU-MISO-OFDM communication systems,” in *Proc. IEEE Wireless Commun. Netw. Conf.*, 2020, pp. 1–6.
- [16] Q. Wu, S. Zhang, B. Zheng, C. You, and R. Zhang, “Intelligent reflecting surface-aided wireless communications: A tutorial,” *IEEE Trans. Commun.*, vol. 69, no. 5, pp. 3313–3351, 2021.
- [17] J. Zhao, “A survey of intelligent reflecting surfaces (IRSs): Towards 6G wireless communication networks,” *arXiv preprint arXiv:1907.04789*, 2019.
- [18] Z. Chen, X. Ma, C. Han, and Q. Wen, “Towards intelligent reflecting surface empowered 6G terahertz communications: A survey,” *China Commun.*, vol. 18, no. 5, pp. 93–119, 2021.
- [19] D. Mishra and H. Johansson, “Channel estimation and low-complexity beamforming design for passive intelligent surface assisted MISO wireless energy transfer,” in *Proc. IEEE Int. Conf. Acoust. Speech Signal Process.*, 2019, pp. 4659–4663.
- [20] Q.-U.-A. Nadeem, H. Alwazani, A. Kamoun, A. Chaaban, M. Debbah, and M.-S. Alouini, “Intelligent reflecting surface-assisted multi-user MISO communication: Channel estimation and beamforming design,” *IEEE Open J. Commun. Soc.*, vol. 1, pp. 661–680, 2020.
- [21] X. Wei, D. Shen, and L. Dai, “Channel estimation for RIS assisted wireless communications—part I: Fundamentals, solutions, and future opportunities,” *IEEE Commun. Lett.*, vol. 25, no. 5, pp. 1398–1402, 2021.
- [22] ———, “Channel estimation for RIS assisted wireless communications—part II: An improved solution based on double-structured sparsity,” *IEEE Commun. Lett.*, vol. 25, no. 5, pp. 1403–1407, 2021.
- [23] T. Lin, X. Yu, Y. Zhu, and R. Schober, “Channel estimation for IRS-assisted millimeter-wave MIMO systems: Sparsity-inspired approaches,” *arXiv preprint arXiv:2107.11605*, 2021.
- [24] Q. Wu and R. Zhang, “Beamforming optimization for wireless network aided by intelligent reflecting surface with discrete phase shifts,” *IEEE Trans. Commun.*, vol. 68, no. 3, pp. 1838–1851, 2020.
- [25] P. Viswanath, D. Tse, and R. Laroia, “Opportunistic beamforming using dumb antennas,” *IEEE Trans. Inf. Theory*, vol. 48, no. 6, pp. 1277–1294, 2002.
- [26] M. Sharif and B. Hassibi, “On the capacity of MIMO broadcast channels with partial side information,” *IEEE Trans. Inf. Theory*, vol. 51, no. 2, pp. 506–522, 2005.
- [27] A. Asadi and V. Mancuso, “A survey on opportunistic scheduling in wireless communications,” *IEEE Commun. Surveys Tuts.*, vol. 15, no. 4, pp. 1671–1688, 2013.
- [28] A. T. Suresh, N. B. Mehta, and V. Shah, “On optimal timer-based distributed selection for rate-adaptive multi-user diversity systems,” in *Natl. Conf. Commun. (NCC)*. IEEE, 2010, pp. 1–5.
- [29] V. Shah, N. B. Mehta, and R. Yim, “Optimal timer based selection schemes,” *IEEE Trans. Commun.*, vol. 58, no. 6, pp. 1814–1823, 2010.
- [30] M. Kafesaki, N. Shen, S. Tzortzakis, and C. Soukoulis, “Optically switchable and tunable terahertz metamaterials through photoconductivity,” *Journal of Optics*, vol. 14, no. 11, p. 114008, 2012.
- [31] P. Jung, S. Butz, M. Marthaler, M. Fistul, J. Leppäkangas, V. Koshelets, and A. Ustinov, “Multistability and switching in a superconducting metamaterial,” *Nature Communications*, vol. 5, no. 1, pp. 1–6, 2014.
- [32] E. Dahlman, S. Parkvall, and J. Sköld, *5G NR: The next generation wireless access technology*. Academic Press, 2020.
- [33] Q.-U.-A. Nadeem, A. Zappone, and A. Chaaban, “Intelligent reflecting surface enabled random rotations scheme for the MISO broadcast channel,” *IEEE Trans. Wireless Commun.*, vol. 20, no. 8, pp. 5226–5242, 2021.
- [34] G. Tian and R. Song, “Cooperative beamforming for a double-IRS-assisted wireless communication system,” *Eurasip J. Adv. Signal Process.*, vol. 2021, no. 1, pp. 1–10, 2021.
- [35] D. Tse and P. Viswanath, *Fundamentals of wireless communication*. Cambridge university press, 2005.
- [36] B. Zheng and R. Zhang, “Intelligent reflecting surface-enhanced OFDM: Channel estimation and reflection optimization,” *IEEE Wireless Commun. Lett.*, vol. 9, no. 4, pp. 518–522, 2020.
- [37] K. D. Katsanos, N. Shlezinger, M. F. Imani, and G. C. Alexandropoulos, “Wideband multi-user MIMO communications with frequency selective IRSs: Element response modeling and sum-rate maximization,” *arXiv preprint arXiv:2202.02169*, 2022.
- [38] O. Eidous and S. Al-Salman, “One-term approximation for normal distribution function,” *Mathematics and Statistics*, vol. 4, no. 1, pp. 15–18, 2016.
- [39] E. Björnson, “Optimizing a binary intelligent reflecting surface for OFDM communications under mutual coupling,” *arXiv preprint arXiv:2106.04280*, 2021.
- [40] K. Najim, E. Ikonen, and A.-K. Daoud, *Stochastic processes: estimation, optimisation and analysis*. Elsevier, 2004.
- [41] P. Billingsley, *Probability and Measure*. 3rd Wiley, 1995.
- [42] B. C. Arnold, N. Balakrishnan, and H. N. Nagaraja, *A first course in order statistics*. SIAM, 2008.
- [43] A. C. Berry, “The accuracy of the gaussian approximation to the sum of independent variates,” *Trans. American Mathematical Society*, vol. 49, no. 1, pp. 122–136, 1941.